Hindawi
Journal of Advanced Transportation
Volume 2022, Article ID 7219741, 15 pages
https://doi.org/10.1155/2022/7219741

Research Article

Overall Influence of Dedicated Lanes for Connected and Autonomous Vehicles on Freeway Heterogeneous Traffic Flow

Yanyan Chen[1], **Hengyi Zhang**[1], **Dongzhu Wang**[2] and **Jiachen Wang**[3]

[1]*Beijing Key Laboratory of Traffic Engineering, Beijing University of Technology, Beijing 100124, China*
[2]*Research Institute of Highway, Ministry of Transport, Beijing 100088, China*
[3]*Beijing University of Technology, Beijing 100124, China*

Correspondence should be addressed to Dongzhu Wang; wangdrew@163.com

Received 10 May 2022; Revised 23 June 2022; Accepted 25 July 2022; Published 24 August 2022

Academic Editor: Fei Hui

With the development of autonomous driving and communication technology, the heterogeneous traffic flow by combining connected and autonomous vehicles (CAVs) and manually driven vehicles (MVs) will appear on the freeway in the near future. It is expected that CAVs can improve the freeway capacity and reduce vehicle exhaust emissions, but sharing the same road by CAVs and MVs will cause certain interference to CAVs. In order to reduce the negative influence of the heterogeneous traffic flow, setting up CAV dedicated lanes to separate CAVs from MVs to a certain extent is regarded as a reasonable solution. Based on the characteristics that MVs should be decelerated by a realistic amplitude and that the connected and autonomous vehicle can accurately predict the speed of its preceding and rear CAVs at the next time step, a heterogeneous traffic flow model was established. Based on this model, we studied the overall influence of different lane strategies on the operating efficiency of freeway traffic flow and vehicle exhaust emissions under different densities with different CAV penetration rates. The results show that setting up CAV dedicated lanes with low CAV penetration rates will have a negative impact on the freeway traffic flow. When the CAV penetration rate is 40%–60% and the density is not less than 30 veh/km/lane, setting up one CAV dedicated lane is the best choice. When the CAV penetration rate exceeds 60% and the density is not less than 40 veh/km/lane, setting up two CAV dedicated lanes is the best choice. The research finding will assist in understanding the overall influence of CAV dedicated lanes on freeway traffic flow and help determine the optimal number of CAV dedicated lanes under different traffic conditions.

1. Introduction

With the continuous and rapid growth of travel demand, the growth of the total freeway mileage is relatively slow due to limited land available [1]. This difference leads to the imbalance between the supply and the demand of freeways, the decrease in road capacity, and the increase in travel time [2]. There is an increasing demand to improve the operating efficiency of freeway traffic flow and reduce vehicle exhaust emissions.

In the past few decades, researchers have been committed to using intelligent transportation systems (ITS) to improve traffic operating efficiency [3–6], ensure traffic safety [7–10], and reduce vehicle exhaust emissions [11–14]. In recent years, with the rapid development of artificial intelligence, sensor, and communication technology, due to the characteristics of autonomous driving, vehicle-to-vehicle (V2V) communication, and vehicle-to-infrastructure (V2I) communication, CAVs have been widely regarded as an effective way to alleviate the traffic problems [15]. However, it is worth noting that the application of CAVs is thought to be a long and slow process [16, 17]. CAVs and MVs will coexist on roads for a long time.

The existing literature contains many contributions made in studying the influence of CAVs on traffic flow under the heterogeneous traffic flow conditions [18–21]. Ioannou and Stefanovic [22] found that adaptive cruise control vehicles could reduce the interference between vehicles, which was beneficial to the environment. Liu et al. [23] studied the influence of the autonomous vehicle (AV) penetration rate

on heterogeneous traffic flow. The results indicated that AVs could considerably improve the traffic condition, and the level of improvement increased with the AV penetration rate. The research also found that the influence of AVs on the heterogeneous traffic flow characteristics was mainly related to the car-following and lane-changing behaviors. Morando et al. [24] estimated the impact of AVs on traffic safety and found that AVs significantly improved traffic safety and reduced the number of conflicts with high AV penetration rates. Gong and Du [25] found that CAVs could stabilize the traffic flow effectively and dampen traffic oscillation propagation. Ye and Yamamoto [26] proposed a heterogeneous traffic flow model including CAVs and MVs. The results showed that, with the increase of the CAV penetration rate, road capacity also increased. Liu et al. [27] studied the influence of cooperative adaptive cruise control (CACC) vehicles on the capacity of the freeway merge bottleneck area. The simulation results indicated that the freeway merge bottleneck area capacity increases quadratically as the penetration rate of CACC vehicles increases. Chen et al. [28] established a heterogeneous traffic flow model of MVs and AVs. The results showed that when the AV penetration rate increases, the critical vehicle density also increases. Zheng et al. [29] studied the stability of heterogeneous traffic flow and found that AVs are able to not only stabilize the traffic flow but also increase the average speed of vehicles effectively. Festa et al. [30] compared the macrosimulation model and the microsimulation model and verified model performances. After that, they [31] proposed an adaptive traffic signal control scheme. Connected vehicles provided their own positions to the control system, and the control system stored the vehicle positions on the network. Meanwhile, new vehicle trajectories were generated based on a map matching algorithm, and a new traffic signal plan was generated. The results showed that the scheme could effectively reduce the average travel time and pollution emissions. Wu et al. [32] established a two-lane lane-changing model and studied the control strategy at the freeway work area under the heterogeneous traffic flow. Their study disclosed that when the CAV penetration rate is high, the combination of the early lane-changing control strategy and the variable speed limits strategy is the optimal choice. Jiang et al. [33] established a heterogeneous traffic flow model based on the analysis of platoon behavior. The results showed that, with the increase of the CAV penetration rate, the road capacity was significantly improved.

Inspired by the managed lane strategy, the CAV dedicated lane strategy is considered to effectively separate CAVs from MVs, realize the local homogeneity of CAVs, and maximize the advantages of CAVs. The managed lane strategy can improve traffic conditions by setting up dedicated lanes for specific vehicles. Bus lanes, high-occupancy vehicle (HOV) lanes, and high-occupancy toll (HOT) lanes are all based on similar concepts and have proven their feasibility through practices [34–36]. Due to the limitations of technologies, studies on the CAV dedicated lane are still at the theoretical level and have not been put into practice.

Mohajerpoor and Ramezani [37] analyzed the total delay of a one-way two-lane road under the heterogeneous traffic flow for different lane allocation strategies. Ghiasi et al. [38] proposed a lane management model for the heterogeneous traffic flow based on the Markov chain method. Based on the condition of providing dedicated lanes for AVs to traffic intersections, Rey and Levin [39] proposed a new traffic signal control strategy. Some scholars have studied the CAV dedicated lane from the perspective of macroscopic network optimization. Chen et al. [40] proposed a mathematical model to optimize the deployment plan of CAV dedicated lanes in the heterogeneous traffic flow network based on time. On the basis of considering the user equilibrium route choice, Melson et al. [41] introduced CACC into the link transmission model (LTM) and found that CACC-dedicated lanes could reduce freeway congestion. By deploying dedicated lanes for AVs and subsidizing people who buy AVs, Chen et al. [42] formulated the AVs incentive program design problem as a stochastic programming model with equilibrium constraints. Some scholars have also studied the influence of CAV dedicated lanes on the traffic flow through microsimulation. Ye and Yamamoto [43] studied the influence of the number of CAV dedicated lanes on the traffic flow throughput. Zhang et al. [44] studied the influence of CAV dedicated lanes on the freeway heterogeneous traffic flow from the perspective of traffic safety. Hua et al. [45] studied the influence of different dedicated lane strategies on the heterogeneous traffic flow. The results showed that the CAV dedicated lanes could improve the freeway capacity, but dedicated lanes for MVs had little impact on the improvement of the freeway capacity.

However, it is worth noting that few researchers have studied the influence of the CAV dedicated lane strategy on vehicle exhaust emissions. This paper aims to evaluate the overall influence of different CAV dedicated lane strategies on the operating efficiency of the freeway traffic flow and vehicle exhaust emissions. We designed three different lane strategies and conducted the simulation under different densities with different CAV penetration rates.

The remainder of this paper is organized as follows. In Section 2, the microsimulation models for CAVs and MVs are established, respectively. In Section 3, different lane strategies are introduced. In Section 4, the simulation results are analyzed, and the optimal ranges of different lane strategies are obtained. Finally, conclusions are obtained with an outline for the future research.

2. Model

The cellular automata model is one of the most widely used micro traffic simulation models [46]. Its advantages of simplicity and flexibility in adapting to the complex characteristics of real traffic flow have been proved in many previous studies. Some typical cellular automata models, including NS model [46], STCA model [47], VDR model [48], KKW model [49, 50], MCD model [51], TS model [52], and TSM model [53], have been proposed. The TSM model can reproduce the metastable state, traffic oscillations, phase transitions, and other real traffic flow dynamics, with significant advantages compared with the other existing models. In this paper, an improved cellular automata model

is proposed based on the TSM model to model the behaviors of MVs. Based on the characteristics of CAVs, the behaviors of CAVs are modeled.

2.1. The Steps Involved in the TSM Model. Step 1: Deterministic speed update

$$\begin{aligned} v_n'(t+1) &= \min\left(v_n(t)+a, v_{\max}, d_{\text{anti}}, v_{\text{safe}}\right),\\ d_{\text{anti}} &= d_n(t) + \max\left(v_{\text{anti}} - g_{\text{safety}}, 0\right),\\ v_{\text{anti}} &= \min\left(d_{n+1}(t), v_{n+1}(t)+a, v_{\max}\right),\\ v_{\text{safe}} &= \left[-b_{\max} + \sqrt{b_{\max}^2 + v_{n+1}^2(t) + 2 * b_{\max} * d_n(t)}\right], \end{aligned} \tag{1}$$

where $v_n(t)$ is the speed of vehicle n at time step t, $v_{\max}$ is the maximum speed of the vehicle, d_{anti} represents the anticipated space gap, v_{safe} denotes the safe speed, $d_n(t)$ is the space gap between vehicle n and its preceding vehicle $n+1$ at time step t, v_{anti} is the expected speed of the preceding vehicle $n+1$ at the next time step $t+1$, $d_{n+1}(t)$ represents the space gap between vehicle $n+1$ and its preceding vehicle at time step t, and $v_{n+1}(t)$ is the speed of vehicle $n+1$ at time step t. In addition, g_{safety}, $b_{\max}$, and a are model parameters, where a and $b_{\max}$ represent vehicle acceleration and maximum deceleration, respectively. $[x]$ denotes the value rounded to its nearest integer.

Step 2: Stochastic deceleration

$$v_n(t+1) = \begin{cases} \max\left(v_n'(t+1) - b_{\text{rand}}, 0\right) \text{with probability } p \\ v_n'(t+1) \text{otherwise} \end{cases},$$

$$b_{\text{rand}} = \begin{cases} a \text{ if } v_n(t) < b_{\text{defense}} + \dfrac{d_{\text{anti}}}{T} \\ b_{\text{defense}} \text{otherwise} \end{cases},$$

$$p = \begin{cases} p_a \text{if } v_n(t) = 0 \\ p_b \text{else if } v_n(t) \le \dfrac{d_{\text{anti}}}{T}, \\ p_{\text{defense}} \text{otherwise} \end{cases}$$

$$p_{\text{defense}} = p_b + \frac{p_c}{1 + e^{\beta\left(v_c - v_n(t)\right)}}, \tag{2}$$

where b_{defense}, T, p_a, p_b, and p_c are model parameters. x can return the maximum integer which is not greater than argument x. Probability p_{defense} is represented by the logistic function, and β and v_c represent the steepness and midpoint of the logistic function, respectively.

Step 3: Position update

$$x_n(t+1) = x_n(t) + v_n(t+1), \tag{3}$$

where $x_n(t)$ is the position of vehicle n at time step t.

2.2. Car-Following Model

2.2.1. Car-Following Model for MVs. To ensure the deceleration within a reasonable range at the next step, we revised the TSM model by replacing d_{anti} with d_{anti}/T at the deterministic speed update step. Meanwhile, in order to make the model more realistic, we introduced $t_{n,h}(t) \le 1$ as one of the conditions for selecting the random probability p, and $t_{n,h}(t) = d_n(t)/v_n(t)$ is the time interval for vehicle n to reach the tail of its preceding vehicle $n+1$.

Using the new rules, the model is modified as follows:

Step 1: Deterministic speed update

$$\begin{aligned} v_n'(t+1) &= \min\left(v_n(t)+a, v_{\max}, \frac{d_{\text{anti}}}{T}, v_{\text{safe}}\right),\\ d_{\text{anti}} &= d_n(t) + \max\left(v_{\text{anti}} - g_{\text{safety}}, 0\right),\\ v_{\text{anti}} &= \min\left(d_{n+1}(t), v_{n+1}(t)+a, v_{\max}\right),\\ v_{\text{safe}} &= \left[-b_{\max} + \sqrt{b_{\max}^2 + v_{n+1}^2(t) + 2 * b_{\max} * d_n(t)}\right]. \end{aligned} \tag{4}$$

Step 2: Stochastic deceleration

$$v_n(t+1) = \begin{cases} \max\left(v_n'(t+1) - b_{\text{rand}}, 0\right) \text{with probability } p \\ v_n'(t+1) \text{otherwise} \end{cases},$$

$$b_{\text{rand}} = \begin{cases} a \text{ if } v_n(t) < b_{\text{defense}} + \dfrac{d_{\text{anti}}}{T} \\ b_{\text{defense}} \text{otherwise} \end{cases},$$

$$p = \begin{cases} p_a \text{if } v_n(t) = 0 \\ p_b \text{else if } t_{n,h}(t) \le 1, \\ p_{\text{defense}} \text{otherwise} \end{cases}$$

$$t_{n,h}(t) = \frac{d_n(t)}{v_n(t)},$$

$$p_{\text{defense}} = p_b + \frac{p_c}{1 + e^{\beta\left(v_c - v_n(t)\right)}}. \tag{5}$$

Step 3: Position update

Table 1: Parameters for the vehicle emission model.

Pollutant	E_0	f_1	f_2	f_3	f_4	f_5	f_6
CO_2	0	5.53×10^{-1}	1.61×10^{-1}	-2.89×10^{-3}	2.66×10^{-1}	5.11×10^{-1}	1.83×10^{-1}
$NO_X\,(a_n(t) \geq -0.5\,\mathrm{m/s^2})$	0	6.19×10^{-4}	8.00×10^{-5}	-4.03×10^{-6}	-4.13×10^{-4}	3.80×10^{-4}	1.77×10^{-4}
$NO_X\,(a_n(t) \geq -0.5\,\mathrm{m/s^2})$	0	2.17×10^{-4}	0	0	0	0	0
$VOC\,(a_n(t) \geq -0.5\,\mathrm{m/s^2})$	0	4.47×10^{-3}	7.32×10^{-7}	-2.87×10^{-8}	-3.41×10^{-6}	4.94×10^{-6}	1.66×10^{-6}
$VOC\,(a_n(t) \geq -0.5\,\mathrm{m/s^2})$	0	2.63×10^{-3}	0	0	0	0	0

$$x_n(t+1) = x_n(t) + v_n(t+1). \tag{6}$$

2.2.2. Car-Following Model for CAVs. Based on the TSM model and the characteristics of CAVs, the car-following model based on the autonomous driving and communication technology is established.

$$v_n(t+1) = \min\left(v_n(t) + a_n(t), v_{\max}, d_{\text{anti}}, v_{\text{safe}}\right), \tag{7}$$

where $a_n(t)$ is the acceleration of vehicle n at time step t, which is defined by the adaptive cruise control model [54].

$$\begin{aligned} a_n(t) &= \max\left(\min\left(a_1, a_{\max}\right), -b_{\max}\right), \\ a_1 &= K_1\left(d_n(t) - v_n(t) * T_{\text{ACC}}\right) + K_2\left(v_{n+1}(t) - v_n(t)\right), \end{aligned} \tag{8}$$

where $a_{\max}$, T_{ACC}, K_1, and K_2 are model parameters. T_{ACC} represents the desired net time gap of vehicle n relative to its preceding vehicle, and $a_{\max}$ represents the maximum acceleration of the vehicle.

When the preceding vehicle $n+1$ is an MV, since the speed of vehicle $n+1$ at the next time step $t+1$ cannot be accurately obtained, the anticipated space gap d_{anti} of the current vehicle n is defined as

$$d_{\text{anti}} = d_n(t). \tag{9}$$

When the preceding vehicle $n+1$ is a CAV, the anticipated space gap d_{anti} of the current vehicle n is defined as

$$d_{\text{anti}} = d_n(t) + v_{n+1}(t+1), \tag{10}$$

where $v_{n+1}(t+1)$ is the anticipated speed of the preceding vehicle $n+1$ at the next time step $t+1$, since vehicle n can effectively obtain the driving information of vehicle $n+1$, and $v_{n+1}(t+1)$ can be expressed as

$$v_{n+1}(t+1) = \min\left(v_{n+1}(t) + a_{n+1}(t), v_{\max}, d_{\text{anti}}^{n+1}, v_{\text{safe}}^{n+1}\right), \tag{11}$$

where $a_{n+1}(t)$, v_{safe}^{n+1}, and d_{anti}^{n+1} are the acceleration, the safe speed, and the anticipated space gap of vehicle $n+1$ at time step t, respectively. The calculation for d_{anti}^{n+1} is similar to that of d_{anti}. The iteration continues until an MV appears. If i vehicles in front of the current vehicle n are all CAVs, the anticipated speed of the i th vehicle in front of vehicle n at the next time step $t+1$ is

$$\begin{aligned} v_{n+i}(t+1) &= \min\left(v_{n+i}(t) + a_{n+i}(t), v_{\max}, d_{\text{anti}}^{n+i}, v_{\text{safe}}^{n+i}\right), \\ d_{\text{anti}}^{n+i} &= d_{n+i}(t), \end{aligned} \tag{12}$$

Table 2: Parameters for the heterogeneous traffic flow model.

Parameter	Value
L_{cell}	0.5 m
L_{veh}	15 L_{cell}
a	2 $L_{\text{cell}}/\text{s}^2$
$v_{\max}$	60 L_{cell}/s
T	1.8 s
g_{safety}	20 L_{cell}
$b_{\max}$	6 $L_{\text{cell}}/\text{s}^2$
b_{defense}	2 $L_{\text{cell}}/\text{s}^2$
p_a	0.52
p_b	0.1
p_c	0.85
β	10 s/L_{cell}
v_c	30 L_{cell}/s
$a_{\max}$	6 $L_{\text{cell}}/\text{s}^2$
K_1	$0.14\,\text{s}^{-2}$
K_2	$0.9\,\text{s}^{-1}$
T_{ACC}	1.1 s
p_{lc}^{HDV}	0.2
p_{lc}^{CAV}	1
i	5

where $v_{n+i}(t)$ represents the speed of vehicle $n+i$ at the time step t, $a_{n+i}(t)$ represents the acceleration of vehicle $n+i$ at the time step t, d_{anti}^{n+i} represents the anticipated space gap of vehicle $n+i$, $d_{n+i}(t)$ is the space gap between vehicle $n+i$ and its preceding vehicle $n+i+1$ at the time step t, and v_{safe}^{n+i} is the safe speed of vehicle $n+i$.

For CAVs, since their reaction time is assumed to be 0, the safe speed can be defined as

$$v_{\text{safe}} = \left\lfloor \sqrt{v_{n+1}^2(t) + 2 * b_{\max} * d_n(t)} \right\rfloor. \tag{13}$$

Finally, the position of vehicle n is updated as follows:

$$x_n(t+1) = x_n(t) + v_n(t+1). \tag{14}$$

2.3. Lane-Changing Model. Vehicles preferentially select the left lane as the target lane in general. For MVs, they can only travel along general lanes. CAVs can travel along all lanes.

2.3.1. Lane-Changing Model for MVs. When the following conditions are met, an MV will move onto the target lane with a probability of p_{lc}^{HDV}.

Step 1: The motivational conditions

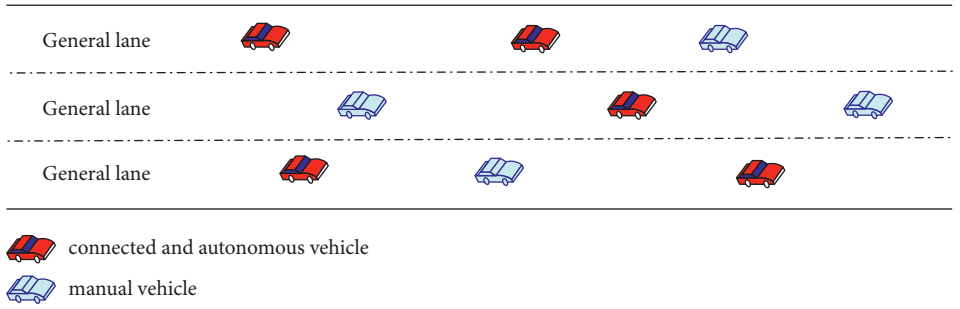

Figure 1: The basic scenario.

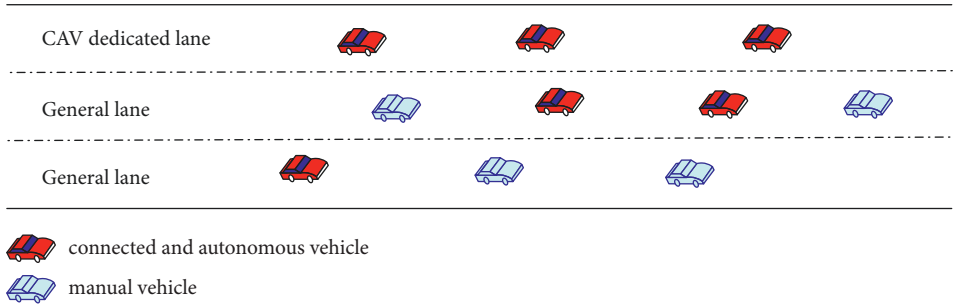

Figure 2: The scenario of one CAV dedicated lane.

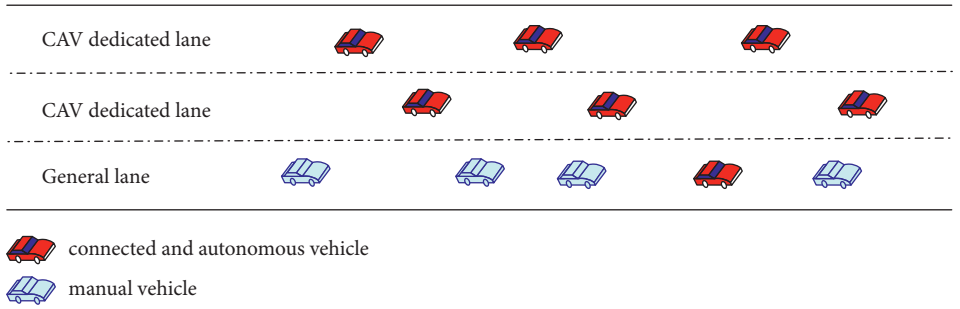

Figure 3: The scenario of two CAV dedicated lanes.

$$\begin{aligned} &d_n(t) < \min\left(v_n(t) + 1, v_{\max}\right), \\ &d_{\text{other}}(t) > d_n(t), \\ &d_{\text{other}}(t) = d_n^{\text{other}}(t). \end{aligned} \tag{15}$$

Step 2: The safety condition

$$d_{\text{other}}^{\text{back}}(t) > v_{\max}, \tag{16}$$

where $d_{\text{other}}(t)$ is the anticipated space gap between vehicle n and the preceding vehicle on the target lane at the time step t, $d_n^{\text{other}}(t)$ is the space gap between vehicle n and the preceding vehicle on the target lane at the time step t, and $d_{\text{other}}^{\text{back}}(t)$ is the space gap between vehicle n and the rear vehicle on the target lane at the time step t.

2.3.2. Lane-Changing Model for CAVs. When the following conditions are met, a CAV will move onto the target lane with a probability of p_{lc}^{CAV}.

Step 1: The motivational conditions

$$\begin{aligned} &d_{\text{anti}} < \min\left(v_n(t) + a_n(t), v_{\max}\right), \\ &d_{\text{other}}(t) > d_{\text{anti}}. \end{aligned} \tag{17}$$

When the preceding vehicle on the current lane is a CAV, d_{anti} can be defined as

$$d_{\text{anti}} = d_n(t) + v_{n+1}(t+1). \tag{18}$$

When the preceding vehicle on the current lane is an MV, d_{anti} can be defined as

$$d_{\text{anti}} = d_n(t). \tag{19}$$

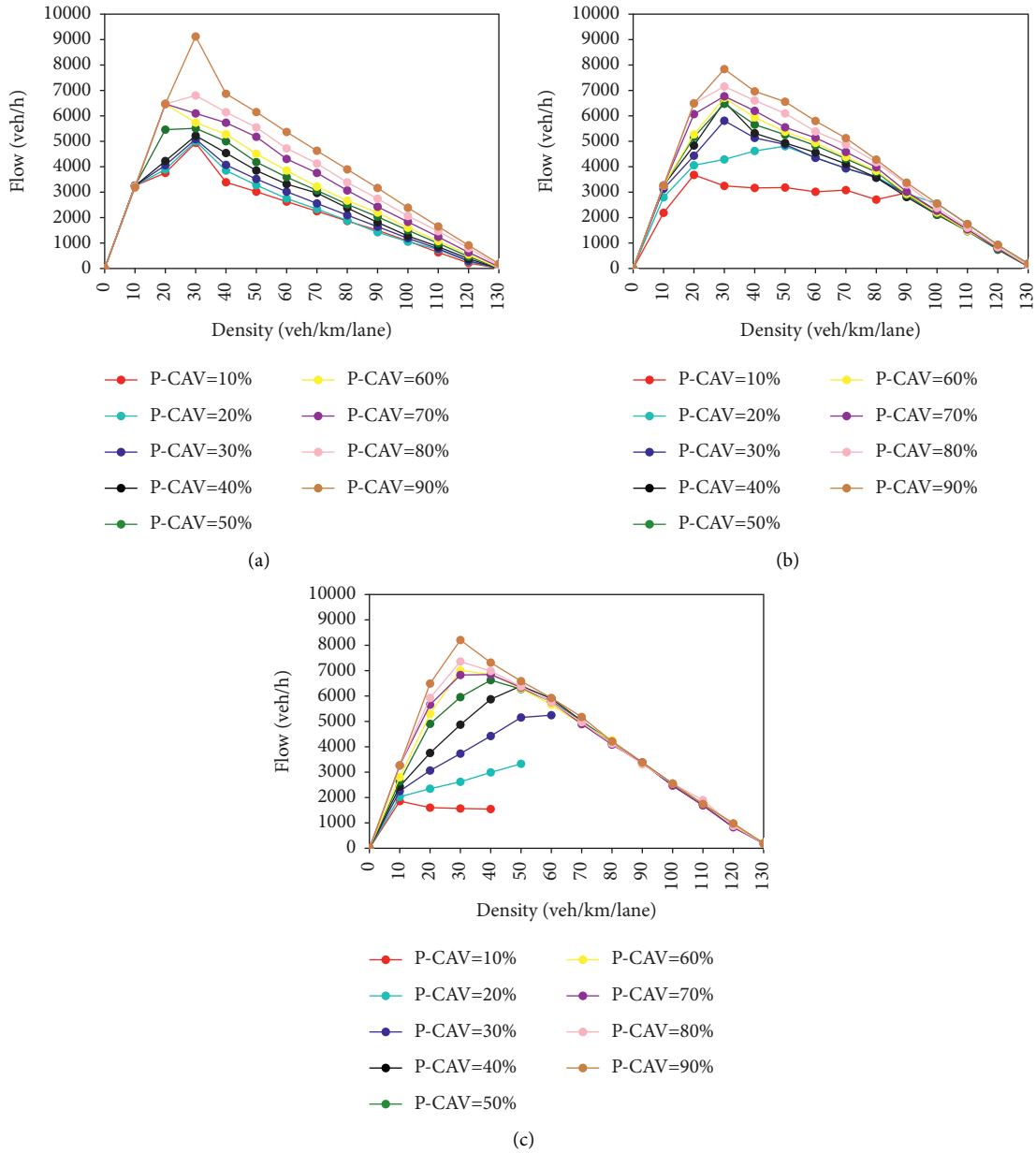

Figure 4: Flow-density diagrams under different C[[parms resize(1),pos(50,50),size(200,200),bgcol(156)]]netration rates. (a) The basic scenario. (b) The scenario of one CAV dedicated lane. (c) The scenario of two CAV dedicated lanes.

When the preceding vehicle on the target lane is a CAV, $d_{\text{other}}(t)$ can be defined as

$$d_{\text{other}}(t) = d_n^{\text{other}}(t) + v_{n+1}^{\text{other}}(t+1), \tag{20}$$

where $v_{n+1}^{\text{other}}(t+1)$ represents the anticipated speed of the preceding vehicle on the target lane at the next time step $t+1$.

When the preceding vehicle on the target lane is an MV, $d_{\text{other}}(t)$ can be defined as

$$d_{\text{other}}(t) = d_n^{\text{other}}(t). \tag{21}$$

Step 2: The safety condition

When the rear vehicle on the target lane is a CAV, the safety condition is as follows:

$$d_{\text{other}}^{\text{back}}(t) > v_{n-1}^{\text{other}}(t+1), \tag{22}$$

where $v_{n-1}^{\text{other}}(t+1)$ represents the anticipated speed of the rear vehicle on the target lane at the next time step $t+1$.

When the rear vehicle on the target lane is an MV, the safety condition is as follows:

$$d_{\text{other}}^{\text{back}}(t) > v_{\max}. \tag{23}$$

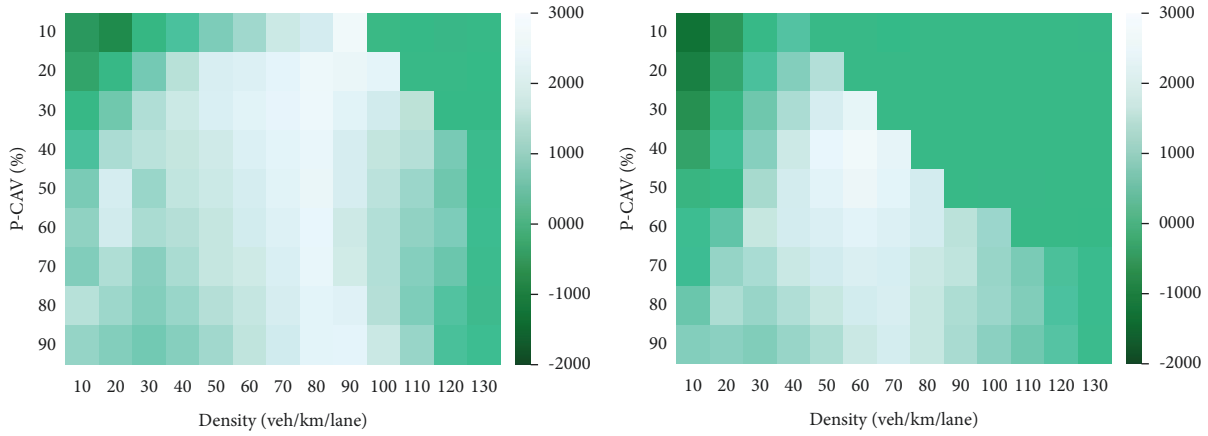

Figure 5: Average capacity difference between CAV dedicated lanes and general lanes. (a) The scenario of one CAV dedicated lane. (b) The scenario of two CAV dedicated lanes.

2.4. Vehicle Exhaust Emission Model. Based on the collected data, Panis et al. [55] established a vehicle exhaust emission model by using the nonlinear multiple regression technique. The model is related to the instantaneous speed and acceleration of the vehicle and suitable for estimating the vehicle exhaust emissions on the freeway. Emission $E_n(t)$ of vehicle n at the time step t is defined as follows:

$$E_n(t) = \max\left[E_0, f_1 + f_2 v_n(t) + f_3 v_n^2(t) + f_4 a_n(t) + f_5 a_n^2(t) + f_6 v_n(t) a_n(t)\right], \tag{24}$$

where E_0 represents the lower limit of vehicle emissions corresponding to the specified emission type and f_1 to f_6 represent the parameters corresponding to each vehicle type and emission type, respectively. $v_n(t)$ and $a_n(t)$ represent the instantaneous speed and acceleration of vehicle n at time step t, respectively. The model parameters are shown in Table 1 [55].

3. Scenarios

In this paper, the cellular automata model is used to establish the simulation environment for a one-way three-lane freeway segment. The parameter values of the heterogeneous traffic flow model are shown in Table 2 [26, 28, 53]. The length of the cell is set to be 0.5 m. Each lane is represented by 5000 cells; that is, the lane length is 2500 m. The length of the vehicle is set as 7.5 m; in other words, each vehicle occupies 15 cells. The boundary condition is set as the periodical boundary condition. Each simulation runs 5600 time steps: the first 2000 time steps will be deleted and only the last 3600 time steps will be retained, representing about a 60-minute run. The simulation results will be analyzed in Section 4.

3.1. The Basic Scenario. In the basic scenario, there is no CAV dedicated lane on the freeway, and CAVs and MVs can travel along all lanes, as shown in Figure 1.

3.2. One CAV Dedicated Lane Scenario. In the initial stage, with the increase of the CAV penetration rate, the innermost lane will be transformed into a CAV dedicated lane, as shown in Figure 2. On the CAV dedicated lane, since there is no interference from MVs, the adjacent CAVs can exchange their speed and position information to maintain a high average speed.

3.3. Two CAV Dedicated Lanes Scenario. With the further increase of the CAV penetration rate, two CAV dedicated lanes will be set up, as shown in Figure 3. This strategy will further increase the right of way of CAVs, reduce the interference of the heterogeneous traffic flow on CAVs, and maximize the advantages of CAVs.

4. The Simulation Results

This section discusses the situations where different CAV dedicated lane strategies are best suitable for five aspects: flow, speed, CO_2 emissions, NO_X emissions, and VOC emissions. Under the condition of the same density, the number of vehicles on the freeway is the same no matter whether the CAV dedicated lane is set up on the freeway or not, and therefore the average exhaust emission of vehicles is used instead of exhaust emission value as the evaluation index.

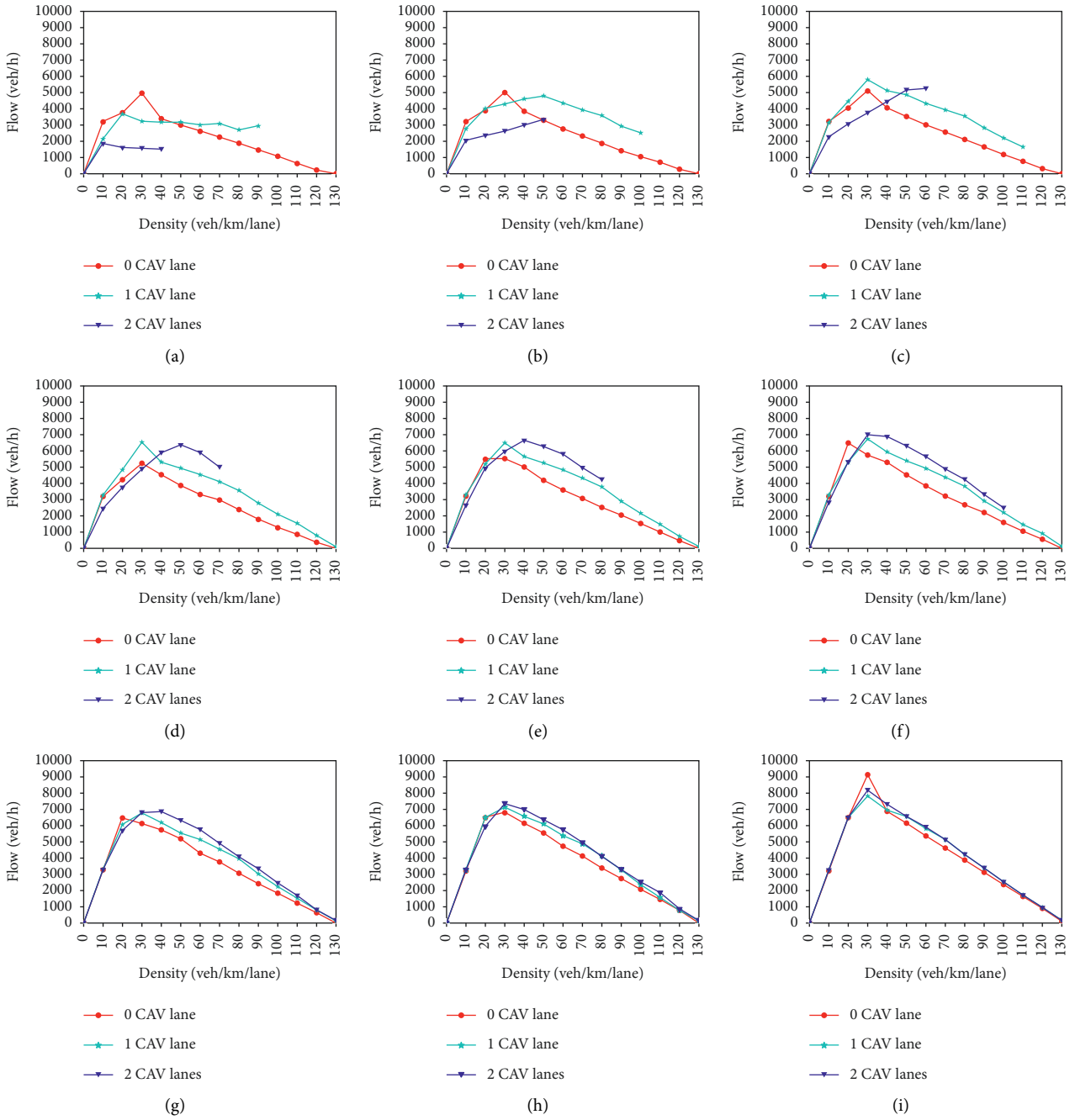

Figure 6: Flow-density diagrams under different CAV penetration rates.

4.1. Flow. Figure 4 shows the relationship between flow and density under different CAV penetration rates in the three scenarios. From Figure 4(a), we can see that when the density is less than 20 veh/km/lane, vehicles are traveling in the state of free flow. For such situation, the CAV penetration rate has a small impact on the road capacity. When the density is 20 veh/km/lane or 30 veh/km/lane, the road capacity reaches the maximum. At this time, with the increase of the CAV penetration rate, the maximum road capacity can increase from 5000 veh/h to 9200 veh/h, indicating that the CAV penetration rate has a significant impact on the road capacity. Because CAVs can accurately obtain the position and speed information of surrounding vehicles through V2V and V2I communication, the driving performance is better than that of MVs. With the increase of the CAV penetration rate, the information available to CAVs also increases, which helps CAVs maintain high speed, thus improving the road capacity. With the further increase of the density, the road capacity begins to decline. However, compared with the road capacity under the conditions of low CAV penetration rates, the road capacity declines more slowly under the conditions of high CAV penetration rates.

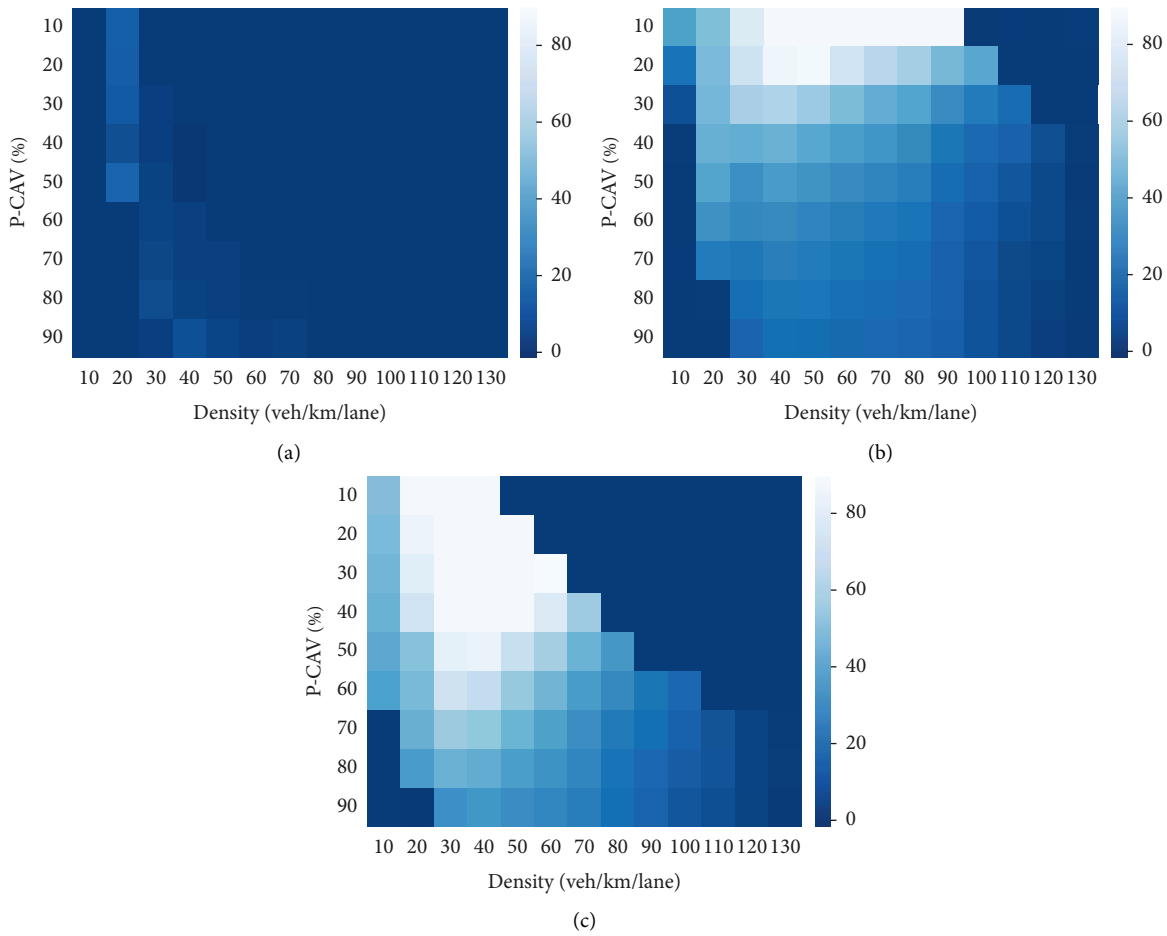

Figure 7: Average speed difference between CAVs and MVs. (a) The basic scenario. (b) The scenario of one CAV dedicated lane. (c) The scenario of two CAV dedicated lanes.

Meanwhile, the higher road capacity can be maintained in a wider density range with the increase of CAV penetration rate. As shown in Figures 4(b) and 4(c), under the conditions of low CAV penetration rates, freeways with one or two CAV dedicated lanes have lower road capacity. This is mainly due to the fact that there are few CAVs on the freeway; setting up CAV dedicated lanes at this time causes the imbalance in the distribution of road resources. Therefore, under the conditions of low CAV penetration rates, it is inappropriate to set up CAV dedicated lanes on the freeway.

As can be seen from Figures 5(a) and 5(b), under the conditions of low densities and low CAV penetration rates, the average capacity of the CAV dedicated lanes is less than that of general lanes. This is because vehicles are in the state of free flow under the low-density conditions. At this time, due to the low CAV penetration rate, the number of vehicles on the CAV dedicated lanes is too small and therefore the capacity is small. As the density and the CAV penetration rate increase, the average capacity of the CAV dedicated lanes increases and exceeds that of general lanes. The maximum average capacity difference can exceed 2000 veh/h. This shows that setting up the CAV dedicated lanes can significantly improve the capacity of the CAV dedicated lanes, but its negative impact on general lanes also should not be ignored. Setting up the CAV dedicated lanes will compress the road space for MVs and reduce the capacity of the general lanes. In order to evaluate the influence of the CAV dedicated lanes on the freeway traffic flow, we should consider not only the improvement of traffic conditions of the CAV dedicated lanes but also the improvement of the overall traffic flow. Therefore, we illustrate the flow-density relationship under the different CAV penetration rates in Figure 6.

As can be seen from Figure 6, the traffic flow under different lane strategies is significantly different. When the CAV penetration rate is 10%, on the whole, the strategy that does not set up the CAV dedicated lanes on the freeway is most beneficial to traffic flow. When the CAV penetration rate is 20% and the density exceeds 40 veh/km/lane, the traffic flow of the freeway with one CAV dedicated lane is higher than that of the freeway without the CAV dedicated lanes. However, the maximum traffic flow of the freeway with one CAV dedicated lane is lower than that of the freeway without the CAV

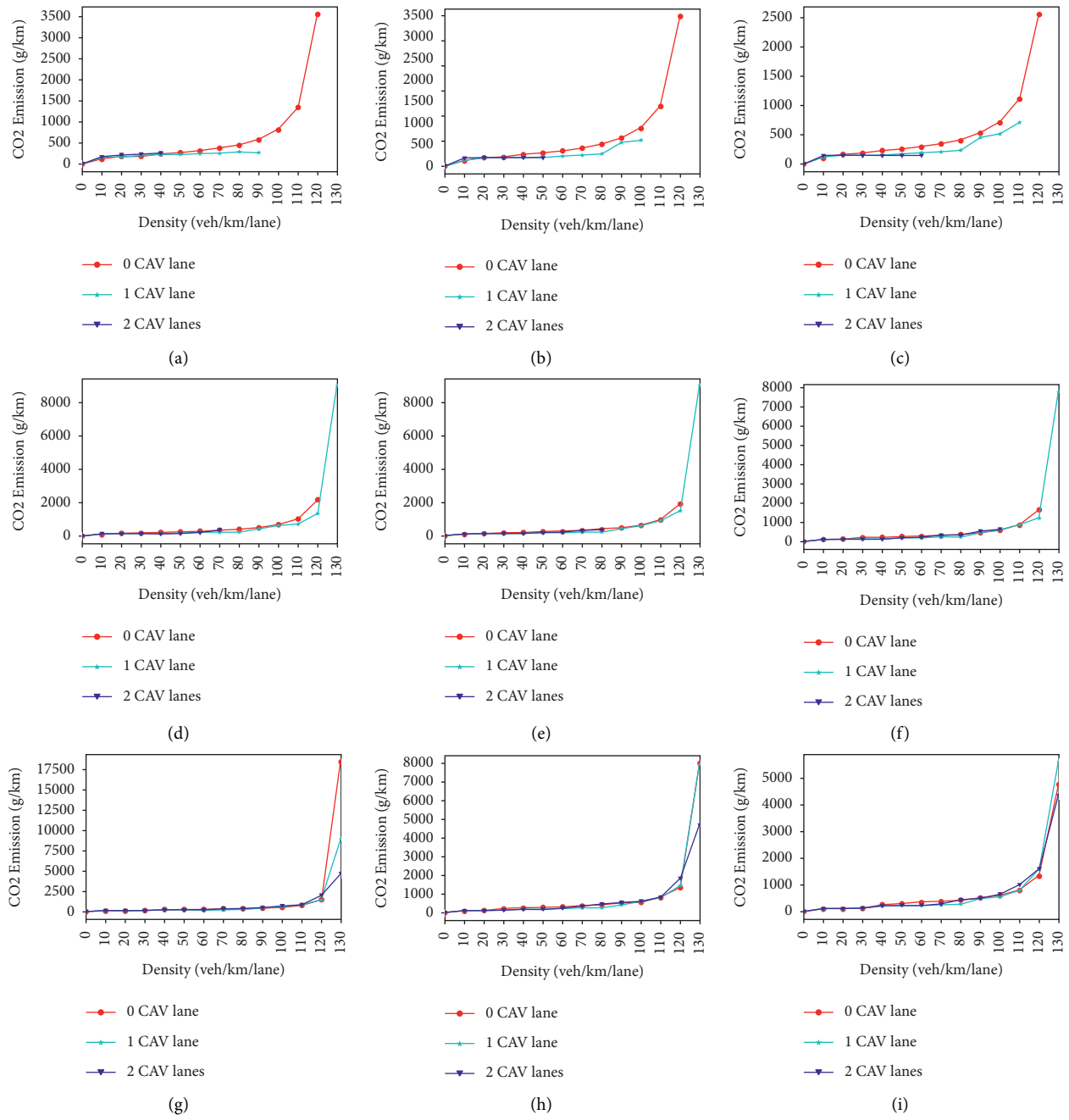

Figure 8: CO_2 emissions-density diagrams under different CAV penetration rates. (a) P-CAV = 10%. (b) P-CAV = 20%. (c) P-CAV = 30%. (d) P-CAV = 40%. (e) P-CAV = 50%. (f) P-CAV = 60%. (g) P-CAV = 70%. (h) P-CAV = 80%. (i) P-CAV = 90%.

dedicated lanes. When the CAV penetration rate is 30%, on the whole, the strategy that sets up one CAV dedicated lane on the freeway is most beneficial to traffic flow. However, due to the low CAV penetration rate, when the density is not less than 120 veh/km/lane, it is impossible to set up one CAV dedicated lane on the freeway, because this will cause the general lanes to be unable to accommodate all MVs. When the CAV penetration rate exceeds 30% and the density is not less than 30 veh/km/lane, the overall traffic flow performance of the freeway with one CAV dedicated lane is better than that of the freeway without the CAV dedicated lanes. Similarly, when the CAV penetration rate exceeds 60% and the density is not less than 40 veh/km/lane, the overall traffic flow performance of the freeway with two CAV dedicated lanes is best. Meanwhile, with the increase of the CAV penetration rate, the variation of traffic flow resulting from different lane strategies decreases. This shows that, under the conditions of high CAV penetration rates, the heterogeneous traffic flow has little interference to CAVs and the influence of CAV dedicated lanes on traffic flow is weakened.

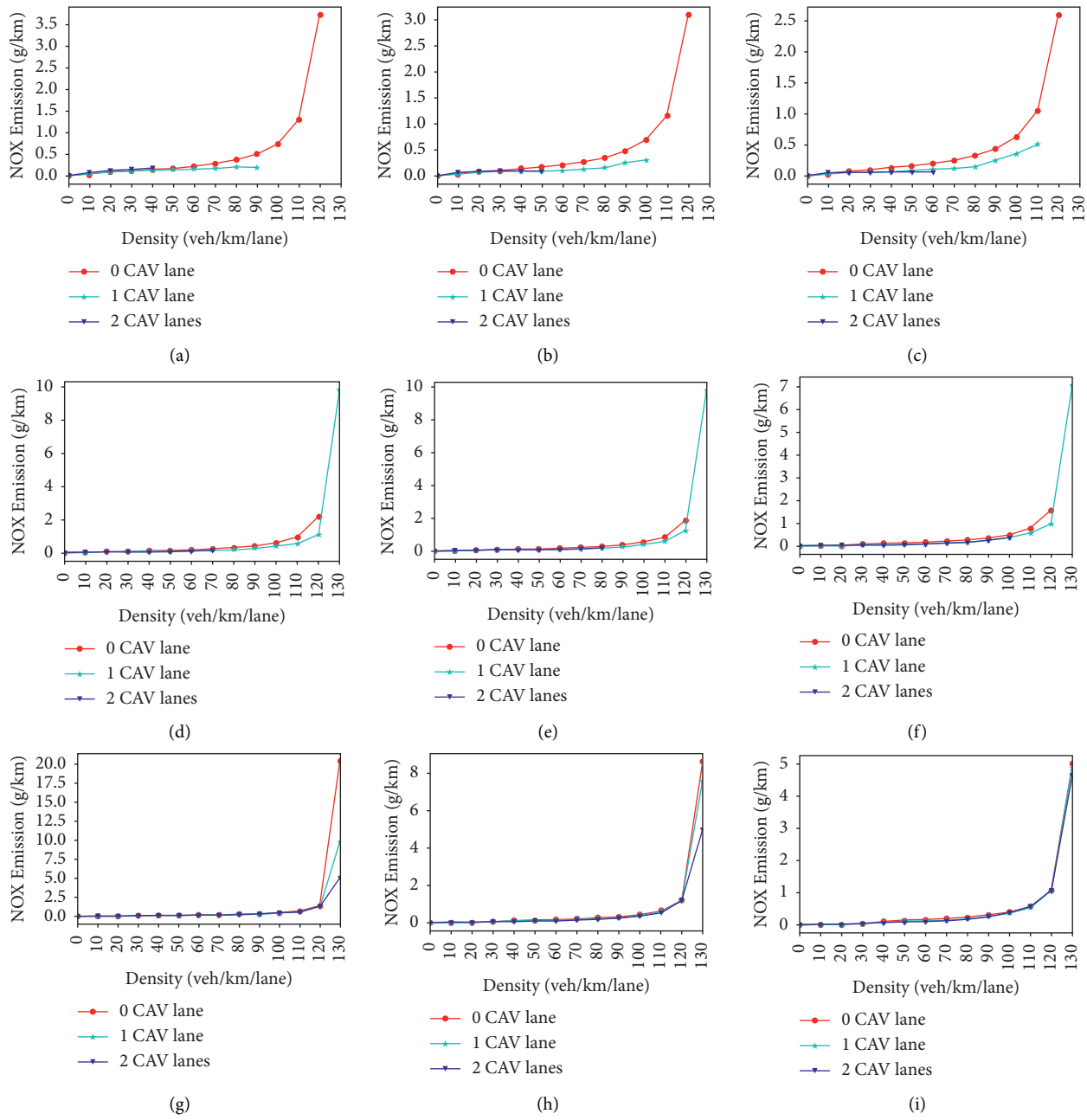

Figure 9: NO_X emissions-density diagrams under different CAV penetration rates. (a) P-CAV = 10%. (b) P-CAV = 20%. (c) P-CAV = 30%. (d) P-CAV = 40%. (e) P-CAV = 50%. (f) P-CAV = 60%. (g) P-CAV = 70%. (h) P-CAV = 80%. (i) P-CAV = 90%.

4.2. Speed. Comparing Figures 7(a)–7(c), we can see that the heterogeneous traffic flow has a significant impact on CAVs. In the basic scenario, because there is no dedicated lane for CAVs, the phenomenon of mixed traffic is very serious. At this time, under the conditions of different densities and CAV penetration rates, the average speed of CAVs is close to that of MVs. From Figures 7(b) and 7(c), it can be seen that the CAV dedicated lane effectively alleviates the phenomenon of mixed traffic. The average speed of CAVs is significantly higher than that of MVs.

4.3. CO_2 Emissions. It can be seen from Figures 8(a)–8(c) that, under the conditions of low CAV penetration rates, when the density exceeds 50 veh/km/lane, setting up the CAV dedicated lanes can effectively reduce CO_2 emissions. At this time, setting up the CAV dedicated lanes can effectively separate CAVs from MVs and reduce the interference caused by uncertain driving behaviors of MVs to CAVs, thereby reducing acceleration and deceleration behaviors of vehicles, and thus reduce CO_2 emissions. As can be seen from Figures 8(d)–8(g), when the CAV penetration

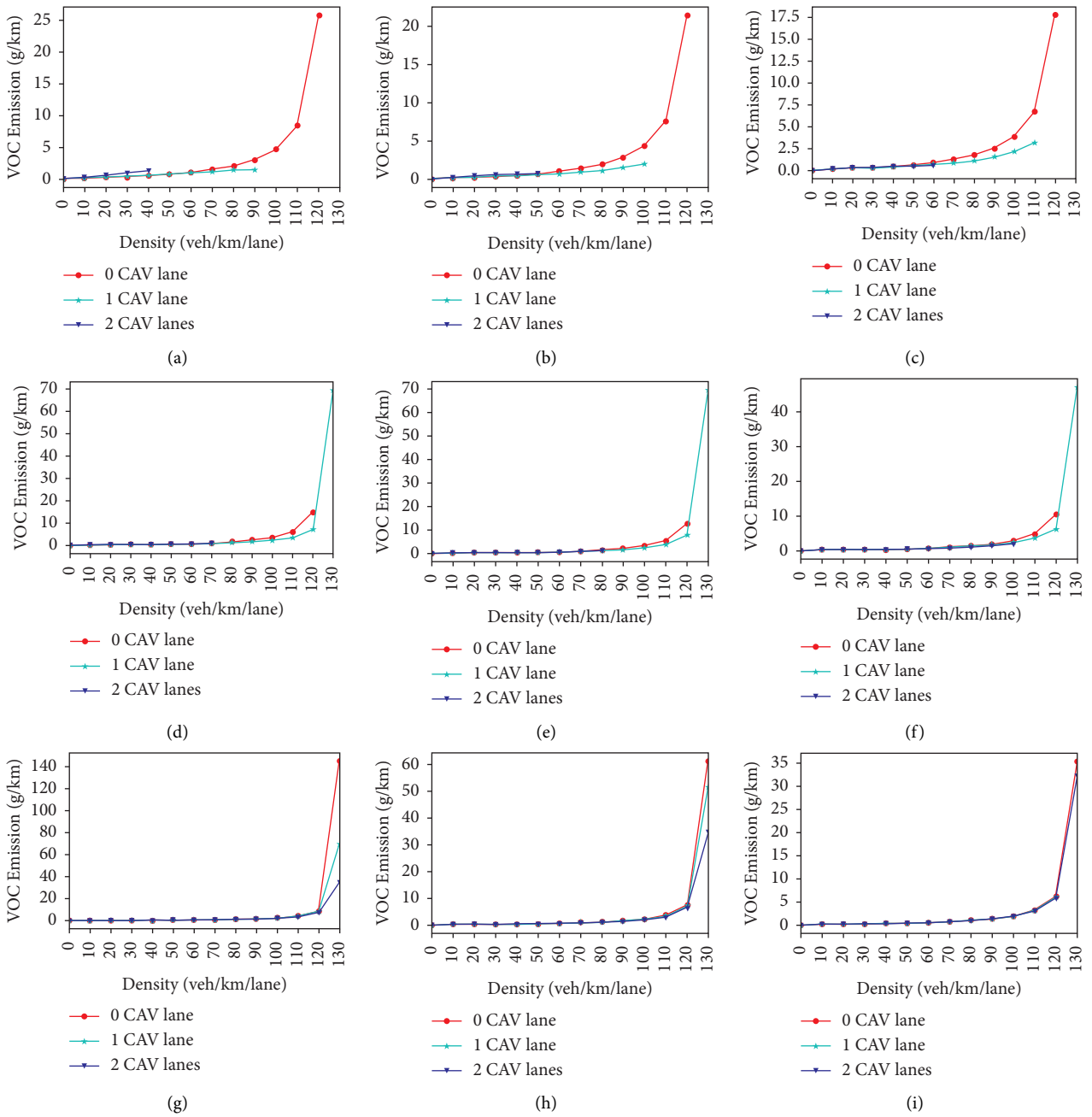

Figure 10: VOC emissions-density diagrams under different CAV penetration rates. (a) P-CAV = 10%. (b) P-CAV = 20%. (c) P-CAV = 30%. (d) P-CAV = 40%. (e) P-CAV = 50%. (f) P-CAV = 60%. (g) P-CAV = 70%. (h) P-CAV = 80%. (i) P-CAV = 90%.

rate is 40%–70%, CO_2 emissions under different lane strategies are similar under the medium-density conditions (40 veh/km/lane–100 veh/km/lane). At this time, although the freeway sets up one or two CAV dedicated lanes, due to the many opportunities for vehicles to change lanes, the vehicle acceleration and deceleration actions are frequent and therefore the difference between CO_2 emissions under different lane strategies is small. From Figures 8(h)–8(i), we can see that when the CAV penetration rate exceeds 70%, under the medium-density conditions (40 veh/km/lane–100 veh/km/lane), setting up CAV dedicated lanes can reduce CO_2 emissions. At this time, there are a large number of CAVs on the freeway, and setting up the CAV dedicated lanes is conducive to the coordinated driving of CAVs, which enhances the stability of traffic flow and avoids frequent acceleration and deceleration behaviors of vehicles, thus reducing CO_2 emissions.

4.4. NO_X and VOC Emissions. As can be seen from Figures 9 and 10, on the whole, setting up the CAV dedicated lanes can effectively reduce NO_X and VOC emissions. This is because setting up the CAV dedicated lanes can significantly reduce the interference between CAVs and MVs, which is

conducive to maximizing the advantages of CAVs, reducing the frequent acceleration and deceleration, and consequently reducing NO_X and VOC emissions. Specifically, when the CAV penetration rate exceeds 30%, on the whole, the emissions of NO_X and VOC of the freeway with one CAV dedicated lane are lower than those of the freeway with no CAV dedicated lane. Similarly, when the CAV penetration rate exceeds 60%, the emissions of NO_X and VOC of the freeway with two CAV dedicated lanes are the lowest.

5. Conclusions

In this paper, a heterogeneous traffic flow model is established to study the overall influence of the CAV dedicated lane on the freeway traffic flow. The model is mainly improved from the two following points: one is that MVs should be decelerated by a realistic amplitude and the other is that CAVs can accurately predict the speed of its preceding and rear CAVs at the next time step. Under different densities and CAV penetration rates, we studied the flow, speed, CO_2 emissions, NO_X emissions, and VOC emissions under different lane strategies by a set of numerical simulations. The simulation results show that the density and the CAV penetration rate have significant impacts on the performance of the CAV dedicated lane strategy. Under the conditions with low CAV penetration rates, setting up the CAV dedicated lanes has negative impacts on the operating efficiency of traffic flow and vehicle exhaust emissions. When the density is not less than 30 veh/km/lane and the CAV penetration rate is 40%–60%, the lane strategy to set up one CAV dedicated lane is the best choice. When the density is not less than 40 veh/km/lane and the CAV penetration rate exceeds 60%, the lane strategy to set up two CAV dedicated lanes is the best choice.

This paper investigates the effect of the traffic density and the CAV penetration rate on the performance of lane-setting strategies. The results are helpful to determine the optimal number of CAV dedicated lanes under different traffic conditions. The established model can be easily extended to other specific scenarios and thus there is significance of the application in the research field of the CAV dedicated lane management strategies in the future. However, there are still some shortcomings in this paper. The influence of CAV dedicated lanes on the merging and diverging area of freeways needs to be studied and analyzed in the future.

Data Availability

The data used to support the findings of this study are available from the corresponding author upon request.

Conflicts of Interest

The authors declare that they have no conflicts of interest.

Authors' Contributions

The authors confirm contributions to the paper as follows: Yanyan Chen and Hengyi Zhang designed the simulation scenarios and received valuable comments and suggestions from Dongzhu Wang in this process. Dongzhu Wang and Hengyi Zhang built the car-following model and lane-changing model of the connected and autonomous vehicle and the manual vehicle. Yanyan Chen and Hengyi Zhang put forward the simulation evaluation indexes and analyzed the simulation results. Jiachen Wang polished the language of the paper.

Acknowledgments

This research was funded by Key Science and Technology Project of the Transportation Industry of the Ministry of Communications, China (2021-ZD2-047), and Transportation Science and Technology Planning Project of Shandong Province, China (2021B49).

References

[1] *Focus on Congestion Relief*, FHWA, 2016.

[2] D. Schrank, B. Eisele, T. Lomax, and J. Bak, *Urban Mobility Scorecard*, Texas A&M Transportation Institute and INRIX, College Station, 2015.

[3] A. Kesting, M. Treiber, and D. Helbing, "Enhanced intelligent driver model to access the impact of driving strategies on traffic capacity," *Philosophical Transactions of the Royal Society A: Mathematical, Physical & Engineering Sciences*, vol. 368, no. 1928, pp. 4585–4605, 2010.

[4] Y. s. Ci, L. n. Wu, X. z. Ling, and Yl Pei, "Operation reliability for on-ramp junction of urban freeway," *Journal of Central South University of Technology*, vol. 18, no. 1, pp. 266–270, 2011.

[5] L. Wu, Y. Ci, Y. Sun, and W. Qi, "Research on joint control of on-ramp metering and mainline speed guidance in the urban expressway based on MPC and connected vehicles," *Journal of Advanced Transportation*, vol. 2020, Article ID 7518087, 2020.

[6] Y. Ci, H. Wu, Y. Sun, and L. Wu, "A prediction model with wavelet neural network optimized by the chicken swarm optimization for on-ramps metering of the urban expressway," *Journal of Intelligent Transportation Systems*, vol. 26, no. 3, pp. 356–365, 2022.

[7] Z. Li, Y. Ci, C. Chen et al., "Investigation of driver injury severities in rural single-vehicle crashes under rain conditions using mixed logit and latent class models," *Accident Analysis & Prevention*, vol. 124, pp. 219–229, 2019.

[8] Z. Li, Q. Wu, Y. Ci, C. Chen, X. Chen, and G. Zhang, "Using latent class Analysis and mixed logit model to explore risk factors on driver injury severity in single-vehicle crashes," *Accident Analysis & Prevention*, vol. 129, pp. 230–240, 2019.

[9] Y. Yang, K. He, Y. p. Wang, Zz Yuan, Yh Yin, and Mz Guo, "Identification of dynamic traffic crash risk for cross-area freeways based on statistical and machine learning methods," *Physica A: Statistical Mechanics and Its Applications*, vol. 595, Article ID 127083.

[10] Y. Yang, K. Wang, Z. Yuan, and D. Liu, "Predicting freeway traffic crash severity using XGBoost-bayesian network model with consideration of features interaction," *Journal of Advanced Transportation*, vol. 2022, pp. 1–16, Article ID 4257865, 2022.

[11] Y. Yang, Z. Yuan, J. Chen, and M. Guo, "Assessment of osculating value method based on entropy weight to transportation energy conservation and emission reduction," *Environmental Engineering and Management Journal*, vol. 16, no. 10, pp. 2413–2423, 2017.

[12] Y. Ci, L. Wu, J. Zhao, Y. Sun, and G. Zhang, "V2I-based car-following modeling and simulation on the signalized intersection," *Physica A: Statistical Mechanics and Its Applications*, vol. 525, pp. 672–679, 2019.

[13] L. Wu, Y. Ci, Y. Wang, and P. Chen, "Fuel consumption at the oversaturated signalized intersection considering queue effects: a case study in Harbin, China," *Energy*, vol. 192, pp. 116654–116659, 2020.

[14] X. Wang, M. Liu, Y. Ci, and Y. Yang, "Effectiveness of driver's bounded rationality and speed guidance on fuel-saving and emissions-reducing at a signalized intersection," *Journal of Cleaner Production*, vol. 325, pp. 1–15, 2021.

[15] R. Hoogendoorn, B. van Arerm, and S. Hoogendoom, "Automated driving, traffic flow efficiency, and human factors: literature review," *Transportation Research Record*, vol. 2422, no. 1, pp. 113–120, 2014.

[16] S. E. Shladover, D. Su, and X. Y. Lu, "Impacts of cooperative adaptive cruise control on freeway traffic flow," *Transportation Research Record*, vol. 2324, no. 1, pp. 63–70, 2012.

[17] J. Santa, A. F. Gómez-Skarmeta, and M. Sánchez-Artigas, "Architecture and evaluation of a unified V2V and V2I communication system based on cellular networks," *Computer Communications*, vol. 31, no. 12, pp. 2850–2861, 2008.

[18] J. Lee, B. B. Park, and I. Yun, "Cumulative travel-time responsive real-time intersection control algorithm in the connected vehicle environment," *Journal of Transportation Engineering*, vol. 139, no. 10, pp. 1020–1029, 2013.

[19] E. Paikari, S. Tahmasseby, and B. Far, "A simulation-based benefit analysis of deploying connected vehicles using dedicated short range communication," in *Proceedings of the 2014 IEEE on Intelligent Vehicles Symposium*, pp. 980–985, Dearborn, MI, USA, June 2014.

[20] A. Talebpour, H. S. Mahmassani, and F. E. Bustamante, "Modeling driver behavior in a connected environment: integrated microscopic simulation of traffic and mobile wireless telecommunication systems," *Transportation Research Record*, vol. 2560, no. 1, pp. 75–86, 2016.

[21] K. Yang, S. I. Guler, and M. Menendez, "Isolated intersection control for various levels of vehicle technology: conventional, connected, and automated vehicles," *Transportation Research Part C: Emerging Technologies*, vol. 72, pp. 109–129, 2016.

[22] P. A. Ioannou and M. Stefanovic, "Evaluation of ACC vehicles in mixed traffic: lane change effects and sensitivity analysis," *IEEE Transactions on Intelligent Transportation Systems*, vol. 6, no. 1, pp. 79–89, 2005.

[23] Y. Liu, J. Guo, J. Taplin, and Y. Wang, "Corrigendum to "characteristic analysis of mixed traffic flow of regular and autonomous vehicles using cellular automata"," *Journal of Advanced Transportation*, vol. 2017, Article ID 2854895, 2017.

[24] M. M. Morando, Q. Tian, L. T. Truong, and H. L. Vu, "Studying the safety impact of autonomous vehicles using simulation-based surrogate safety measures," *Journal of Advanced Transportation*, vol. 2018, p. 11, Article ID 6135183, 2018.

[25] S. Gong and L. Du, "Cooperative platoon control for a mixed traffic flow including human drive vehicles and connected and autonomous vehicles," *Transportation Research Part B: Methodological*, vol. 116, pp. 25–61, 2018.

[26] L. Ye and T. Yamamoto, "Modeling connected and autonomous vehicles in heterogeneous traffic flow," *Physica A: Statistical Mechanics and Its Applications*, vol. 490, pp. 269–277, 2018.

[27] H. Liu, X. D. Kan, S. E. Shladover, X. Y. Lu, and R. E. Ferlis, "Modeling impacts of Cooperative Adaptive Cruise Control on mixed traffic flow in multi-lane freeway facilities," *Transportation Research Part C: Emerging Technologies*, vol. 95, pp. 261–279, 2018.

[28] B. Chen, D. Sun, J. Zhou, W. Wong, and Z. Ding, "A future intelligent traffic system with mixed autonomous vehicles and human-driven vehicles," *Information Sciences*, vol. 529, pp. 59–72, 2020.

[29] Y. Zheng, J. Wang, and K. Li, "Smoothing traffic flow via control of autonomous vehicles," *IEEE Internet of Things Journal*, vol. 7, no. 5, pp. 3882–3896, 2020.

[30] D. C. Festa, G. Longo, G. Mazzulla, and G. Musolino, "Experimental analysis of different simulation models for motorway traffic flow," in *Proceedings of the 2001 IEEE on Intelligent Transportation Systems*, pp. 675–680, Oakland, CA, August 2001.

[31] V. Astarita, V. P. Giofre, D. C. Festa, G. Guido, and A. Vitale, "Floating car data adaptive traffic signals: a description of the first real-time experiment with "connected" vehicles," *Electronics*, vol. 9, no. 1, pp. 114–132, 2020.

[32] W. Wu, R. Sun, A. Ni, Z. Liang, and H. Jia, "Simulation and evaluation of speed and lane-changing advisory of CAVS at work zones in heterogeneous traffic flow," *International Journal of Modern Physics B*, vol. 34, no. 21, Article ID 2050201, 2020.

[33] Y. Jiang, S. Wang, Z. Yao, B. Zhao, and Y. Wang, "A cellular automata model for mixed traffic flow considering the driving behavior of connected automated vehicle platoons," *Physica A: Statistical Mechanics and Its Applications*, vol. 582, Article ID 126262, 2021.

[34] M. E. Bari, M. W. Burris, and C. Huang, "The impact of a toll reduction for truck traffic using SH 130," *Case Studies on Transport Policy*, vol. 3, no. 2, pp. 222–228, 2015.

[35] D. Wu, W. Deng, Y. Song, J. Wang, and D. Kong, "Evaluating operational effects of bus lane with intermittent priority under connected vehicle environments," *Discrete Dynamics in Nature and Society*, vol. 2017, pp. 1–13, Article ID 1659176, 2017.

[36] G. Zang, M. Xu, and Z. Gao, "High-occupancy vehicle lanes and tradable credits scheme for traffic congestion management: a bilevel programming approach," *Promet - Traffic & Transportation*, vol. 30, no. 1, pp. 1–10, 2018.

[37] R. Mohajerpoor and M. Ramezani, "Mixed flow of autonomous and human-driven vehicles: analytical headway modeling and optimal lane management," *Transportation Research Part C: Emerging Technologies*, vol. 109, pp. 194–210, 2019.

[38] A. Ghiasi, O. Hussain, Z. S. Qian, and X. Li, "A mixed traffic capacity analysis and lane management model for connected automated vehicles: a Markov chain method," *Transportation Research Part B: Methodological*, vol. 106, pp. 266–292, 2017.

[39] D. Rey and M. W. Levin, "Blue phase: optimal network traffic control for legacy and autonomous vehicles," *Transportation Research Part B: Methodological*, vol. 130, pp. 105–129, 2019.

[40] Z. Chen, F. He, L. Zhang, and Y. Yin, "Optimal deployment of autonomous vehicle lanes with endogenous market penetration," *Transportation Research Part C: Emerging Technologies*, vol. 72, pp. 143–156, 2016.

[41] C. L. Melson, M. W. Levin, B. E. Hammit, and S. D. Boyles, "Dynamic traffic assignment of cooperative adaptive cruise control," *Transportation Research Part C: Emerging Technologies*, vol. 90, pp. 114–133, 2018.

[42] S. Chen, H. Wang, and Q. Meng, "Designing autonomous vehicle incentive program with uncertain vehicle purchase price," *Transportation Research Part C: Emerging Technologies*, vol. 103, pp. 226–245, 2019.

[43] L. Ye and T. Yamamoto, "Impact of dedicated lanes for connected and autonomous vehicle on traffic flow throughput," *Physica A: Statistical Mechanics and Its Applications*, vol. 512, pp. 588–597, 2018.

[44] J. Zhang, K. Wu, M. Cheng, M. Yang, Y. Cheng, and S. Li, "Safety evaluation for connected and autonomous vehicles' exclusive lanes considering penetrate ratios and impact of trucks using surrogate safety measures," *Journal of Advanced Transportation*, vol. 2020, p. 1, Article ID 5847814, 2020.

[45] X. Hua, W. Yu, W. Wang, and W. Xie, "Influence of lane policies on freeway traffic mixed with manual and connected and autonomous vehicles," *Journal of Advanced Transportation*, vol. 2020, p. 1, Article ID 3968625, 2020.

[46] K. Nagel and M. Schreckenberg, "A cellular automaton model for freeway traffic," *Journal de Physique I*, vol. 2, no. 12, pp. 2221–2229, 1992.

[47] D. Chowdhury, D. E. Wolf, and M. Schreckenberg, "Particle hopping models for two-lane traffic with two kinds of vehicles: effects of lane-changing rules," *Physica A: Statistical Mechanics and Its Applications*, vol. 235, no. 3-4, pp. 417–439, 1997.

[48] R. Barlovic, L. Santen, A. Schadschneider, and M. Schreckenberg, "Metastable states in cellular automata for traffic flow," *The European Physical Journal B*, vol. 5, no. 3, pp. 793–800, 1998.

[49] B. S. Kerner, S. L. Klenov, and D. E. Wolf, "Cellular automata approach to three-phase traffic theory," *Journal of Physics A: Mathematical and General*, vol. 35, no. 47, pp. 9971–10013, 2002.

[50] B. S. Kerner, "Three-phase traffic theory and highway capacity," *Physica A: Statistical Mechanics and Its Applications*, vol. 333, pp. 379–440, 2004.

[51] R. Jiang and Q. S. Wu, "Cellular automata models for synchronized traffic flow," *Journal of Physics A: Mathematical and General*, vol. 36, no. 2, pp. 381–390, 2003.

[52] J. Tian, M. Treiber, S. Ma, B. Jia, and W. Zhang, "Microscopic driving theory with oscillatory congested states: model and empirical verification," *Transportation Research Part B: Methodological*, vol. 71, pp. 138–157, 2015.

[53] J. Tian, G. Li, M. Treiber, R. Jiang, N. Jia, and S. Ma, "Cellular automaton model simulating spatiotemporal patterns, phase transitions and concave growth pattern of oscillations in traffic flow," *Transportation Research Part B: Methodological*, vol. 93, pp. 560–575, 2016.

[54] B. S. Kerner, "Failure of classical traffic flow theories: stochastic highway capacity and automatic driving," *Physica A: Statistical Mechanics and Its Applications*, vol. 450, pp. 700–747, 2016.

[55] L. I Panis, S. B. Roekx, and R. Liu, "Modelling instantaneous traffic emission and the influence of traffic speed limits," *Science of the Total Environment*, vol. 371, no. 1-3, pp. 270–285, 2006.